Sensors & Actuators: B. Chemical 360 (2022) 131661

Contents lists available at ScienceDirect

Sensors and Actuators: B. Chemical

journal homepage: www.elsevier.com/locate/snb

New nanostructures inhibiting human mannose binding lectin identified by a novel surface plasmon resonance assay

Gizem Erol [a,b], Patricia Perez Schmidt [c], Alessia Pancaro [d,e], Javier M. Melo Diaz [f,g], Africa G. Barrientos [h,1], John Porter [h], Laura Polito [c], Michal Szymonik [d], Inge Nelissen [d], Daniel I.R. Spencer [f], Arianna Piotti [a], Marten Beeg [a], Maria-Grazia De Simoni [a], Stefano Fumagalli [a], Marco Gobbi [a,*]

[a] Istituto di Ricerche Farmacologiche Mario Negri IRCCS, Via Mario Negri 2, Milan 20156, Italy
[b] PhD program in Neuroscience, University of Milano-Bicocca, Via Cadore, 48, Monza, MB 20900, Italy
[c] National Research Council, CNR-SCITEC, Via G. Fantoli 16/15, Milan 20138, Italy
[d] Flemish Institute for Technological Research (VITO nv), Health Unit, Boeretang 200, Mol 2400, Belgium
[e] Hasselt University, Advanced Optical Microscopy Centre and Biomedical Research Institute, Agoralaan gebouw C, Diepenbeek 3590, Belgium
[f] Ludger Ltd, Culham Science Centre, Abingdon, Oxfordshire OX14 3EB, UK
[g] Department of Chemistry, Royal College of Surgeons in Ireland, 123 St Stephen's Green, Dublin 2, D02 YN77, Ireland
[h] Midatech Pharma PLC, Oddfellows House, 19 Newport Road, Cardiff CF24 0AA, UK

ARTICLE INFO

Keywords:
Mannose binding lectin
Glycans
Nanoparticles
Surface plasmon resonance

ABSTRACT

Circulating mannose-binding lectin (MBL) plays an important role in the progression of tissue damage caused by ischemic events, an account of its high-affinity, multivalent binding to carbohydrate arrays exposed on damaged endothelium (damage-associated molecular patterns, DAMPS). MBL inhibitors have therefore been proposed as a novel protective therapeutic strategy to prevent secondary injury.

We developed a new, convenient, robust surface plasmon resonance (SPR) assay for in vitro screening of compounds interfering with the binding of native human MBL to an appropriate chip surface functionalized with a pattern of sugar moieties mimicking DAMPS. We also characterized the procedure to regenerate the chip surface after each experimental session, accomplished by sequential cleaning with piranha solution followed by UV exposure. The SPR assay detects the specific binding of human recombinant MBL and native MBL present in human serum, and can identify inhibitors of this binding. We observed inhibitory effects of mannose (IC50 ≅ 5 mM), of a nine mannose residues carrying glycan (IC50 ≅ 0.33 mg/mL, corresponding to ~ 175 μM), and mainly mannose-coated gold nanoparticles (IC50 ≅ 1.1 μg /mL). These in vitro results serve as a basis for testing the protective properties of these molecules/nanoparticles later inthe more expensive and time-consuming studies in cells and animal models of MBL mediated-injuries.

1. Introduction

The interaction between lectins and glycans is fundamental in many physio-pathological processes [1–3]. Glycans are chain-like structures composed of many *monosaccharides* linked by glycosidic bonds. They are the carbohydrate portion of glycoconjugates, such as a glycoprotein, glycolipid, or proteoglycan, and are key players in innate immune responses in all living organisms [4]. Their presence on the cell surface – for example the so-called glycocalyx on the endothelial cells of the vascular lumen – is the basis for the recognition and binding by extrinsic

Abbreviations: **MBL**, mannose binding lectin; **DAMPs**, damage-associated molecular patterns; **PAMPs**, pathogen-associated molecular patterns; **SAM**, self-assembled monolayer; **LP,**, lectin pathway; **rhMBL,**, recombinant human mannose binding lectin; **rhFicolin-1**, recombinant ficolin-1; **SPR,**, surface plasmon resonance; **IC50**, the half-maximal inhibitory concentration; **RU**, resonance units; **K_D**, equilibrium dissociation constant; **GNPs**, gold nanoparticles; **TEM**, transmission electron microscopy; **DLS**, dynamic light scattering.

* Corresponding author.
E-mail address: marco.gobbi@marionegri.it (M. Gobbi).
[1] Present Address: i+Med S.Coop, Parque Tecnológico de Álava, 01510 Vitoria-Gazteiz, Álava, Spain.

https://doi.org/10.1016/j.snb.2022.131661

Available online 5 March 2022

(viral agglutinins, bacterial and plant toxins, etc.) or intrinsic molecules (lectin pathway initiators, etc.) [4]. The lectin pathway (LP) is an activation pathway of the complement system, an arm of innate immunity triggered by lectin proteins, e.g mannose binding lectin (MBL) or ficolins, binding to specific carbohydrates—and carbohydrate patterns— on the surface of pathogens (pathogen-associated molecular patterns, PAMPs) or expressed by damaged self-cells (damage-associated molecular patterns, DAMPs) [5]. While the complement activation consequent to the lectin binding to pathogens has a protective role, the consequences of their binding to DAMPs may be deleterious [6].

Many recent publications indicate that the activators of the LP, particularly mannose-binding lectin (MBL), have a key pathogenic role after myocardial [7,8], renal [9], gastrointestinal [10] and cerebral ischemic injury [11,14,1213]. In all these conditions, MBL appears to contribute to tissue injury, and its genetic deletion or pharmacological inhibition are protective. MBL inhibitors might therefore be promising therapeutic strategies, and reliable in vitro assays are needed to identify them before more time-consuming and expensive studies in cells and in vivo.

The so-called "mannan assay" [15,16] has already been used to examine the binding of monovalent carbohydrates to MBL. However, it requires long incubation and washing steps which may affect the accuracy and precision of the measurements.

Label-free sensors, allowing real-time detection of biomolecular interactions, offer important advantages over ELISA-like approaches and might therefore represent very useful alternatives. Different techniques are available in this regards, including those based, for example, on Surface Plasmon Resonance (SPR), Quartz Crystal Microbalance (QCM), Grating Coupled Interferometry (GCI) and Bio-Layer Interferometry (BLI) technologies. Advantages and limitations of these and other label-free sensors have been recently reviewed [17,18].

SPR is probably the most common and well-established label-free technology. The main application is for the characterization of biomolecular interactions in terms of on and off rates (kinetics) and binding strength (affinity) [19] although its versatility allows many other uses [20–23]. In general, one molecule is immobilized on a sensor chip while the other flows through a microfluidic system over the chip surface.

In order to screen putative MBL binders, a direct SPR design was used at first in which the compounds were flowed onto recombinant MBL immobilized on the sensor chip [12]. However, immobilization of MBL can alter its binding properties so it makes this configuration different from the physiological condition, in which MBL is the circulating protein. Thus we developed a different SPR design to mimic the real conditions more closely [24]. This involved MBL-containing solutions, with or without inhibitors, flowing over a sensor chip coated with mannosylated albumin. This enabled us to identify compounds that could prevent the binding of murine MBL isoforms to immobilized mannose residues. Although it gave satisfactory results with murine MBL, this approach did not work with native human MBL [24] thus limiting its application. The main aim of the present work was therefore to design a novel SPR assay to allow investigation in human serum, supporting translational studies.

After extensive development and characterization to generate suitable functionalized surfaces, we obtained a robust and reliable method to measure the binding of human MBL (in solution) to a mannose-exposing sensor chip, and to identify inhibitors of this binding. We applied this new SPR-based biosensor to show the inhibitory properties of a tri-antennary high-mannose glycan or sugar-coated nanoparticles, which are therefore promising molecules worth further investigating.

2. Materials and methods

2.1. Chemicals and reagents

All chemicals were of analytical grade, used without further purification. All water was double-distilled, supplied in house by a Milli-Q system (Millipore, Bedford, MA, USA). Hydrogen peroxide solution (30% w/w) and D-(+)-mannose were purchased from Merck Millipore (Overijse, Belgium). Tween 20 was from Sigma-Aldrich (Milan, Italy). 2-Mercaptoethanol (14.2 M) and cleaning reagents (0.5% SDS, 50 mM NaOH and 100 mM HCl) were from the ProteOn Regeneration Kit (Bio-Rad, California, USA).

2.2. Biological materials

Recombinant human MBL protein (rhMBL) (9086-MB) and recombinant human Ficolin-1 protein, carrier-free (rhFicolin-1) (4209-FC) were purchased from R&D Systems (Minneapolis, MN, USA). Soybean agglutinin (SBA) unconjugated was purchased from Vector Laboratories (L-1010). Human serum (from male AB clotted whole blood), USA origin, sterile-filtered (H6914) was purchased from Merck Life Science S.r.l. MBL, human, mAb 3E7 (HM2061) was purchased from Hycult Biotech.

MBL-depleted human serum was prepared according to a method described previously [25]. Briefly, a 5 mL column containing 2 mL of mannan-agarose (Sigma-Aldrich, Belgium) as depleting beads was equilibrated with Veronal buffer (Lonza, Allendale, New Jersey, US) containing calcium chloride (3 mM) and magnesium chloride (10 mM). Human serum was passed through the column, and the flow-through was collected. The depletion of MBL was confirmed by Human MBL Quantikine ELISA (DMBL00; R&D Systems, bio-techne Ltd. Abingdon, UK) showing $\geq$ 95% depletion efficiency.

M9 Glycan (High mannose or oligo mannose N glycan with a di-N-acetylglucosamine core and 9 mannose residues) 95% purity, was provided by Ludger Ltd. (Fig. S1).

2.3. Thiol-glyco-derivatives

Synthetic glyco-derives, Man-$EG_6C_{11}S$, Glc-$EG_6C_{11}S$ (Fig. S2) were prepared according to the reference method [26,27] by Midatech (Bilbao Spain) and dissolved in water.

2.4. Synthesis, functionalization and characterization of gold nanoparticles

Gold nanoparticles (GNPs) were synthesized and characterized as previously described [28]. Briefly, sodium citrate (9 mL, 68 mM), $HAuCl_4$ (7.5 mL, 10 mM) and $AgNO_3$ (490 μL, 5.9 mM) were mixed and stirred for 6 min at room temperature. Then the solution was added into 250 mL of boiling water in a 500 mL flask and stirred (750 rpm) for 1 h at 100 °C, allowing the formation of the seeds. The seed solution was cooled to room temperature, 5 mL of glycerol was added, and the solution was left stirring for 10 min

A second mixture of sodium citrate (10 mL, 34 mM), $HAuCl_4$ (7.5 mL, 10 mM) and $AgNO_3$ (426 μL, 5.9 mM) was pre-mixed for 6 min and then added to the seed solution, followed immediately by the addition of hydroquinone (8 mL, 91 mM). The solution was left stirring at 750 rpm for 1 h to age and improve homogeneity.

Synthesized citrate-capped GNPs were purified by centrifuging, using Millipore Amicon Ultra-4 Centrifugal Filter Units, 30KDa cut-off, at 6000 rpm for 4 min and stored as colloidal solution in water (12 mL, Au content 14 mg). These citrate-capped GNPs are stable in water for months, and their core diameter is 14.1 $\pm$ 2.1 nm, determined by transmission electron microscopy *(TEM) images* (Fig. S3). We found no evidence of residual silver on the gold surface, checked by TEM and energy dispersive X-ray.

GNPs were functionalized by capping the metal surface with thiol-glyco-derivatives, exploiting the strong thiol-gold bond and allowing a self-assembled monolayer on the gold surface (Fig. S4). First, 15 μL of 10 μg/mL thiol-glyco-derivatives, Man-$EG_6C_{11}S$ or Glc-$EG_6C_{11}S$, were added to 85 μL of water and 500 μL of citrate-capped GNPs (1.16 mg/mL) were added dropwise to the solution, then shaken overnight at 4 °C

in the dark. The samples were centrifuged at 13000 rpm (16.1 rcf) for 25 min at 15 °C. After centrifugation, the supernatant was removed and the GNPs were re-dispersed in 600 μL of water. This step was repeated three times. After the final cycle the particles were dispersed in 300 μL of water.

Citrate-capped GNPs and glyco-functionalized GNPs were fully characterized by: 1) dynamic light scattering (DLS) and ζ-Potential, to determine their hydrodynamic diameter and assess their colloidal stability (Table 1). DLS was done with a 90 Plus Particle Size Analyzer from Brookhaven Instrument Corporation (Holtsville, NY, USA) operating at 15 mW of a solid-state laser (λ 661 nm), using a 90° scattering angle. The ζ-potential was determined at 25 °C, using the same instrument equipped with an AQ-809 electrode, operating at an applied voltage of 120 V. The ζ-potential was calculated from electrophoretic mobility based on the Smoluchowski theory. 2) UV-Vis spectroscopy to characterize the plasmon band was done with an Agilent 8453 instrument equipped with a disposable cuvette with 1 cm optical path length (Fig. S5) and a concentration of NPs calculated with the Beer-Lambert law. 3) Inductive coupled plasma optical emission spectroscopy (ICP-OES) to analyze the metal content was done with ICP-OES iCAP 6200 Duo upgrade, Thermofisher. Samples were acid-digested on a hotplate with *aqua regia* (HCl: HNO_3 3:1) solution, diluted with water. 4) TEM was done on a specimen prepared by dropping the GNP solution onto supported lacey-carbon copper TEM grids, using a ZEISS LIBRA200FE microscope equipped with an in-column Ω-filter spectrometer/filter, operating at 200 kV (Fig. S3).

2.5. Piranha/UV cleaning and chip surface coating

We recycled used GLC and GLM sensor chips from BioRad, which are coated with a modified alginate polymer layer with a different ligand immobilization capacity, which was removed. For this, the used chips were taken out of the housing (Fig. 1) and their surface was immersed in sequence in SDS (0.5%), NaOH (50 mM) and HCl (100 mM) for a min each, with intermediate washes with water, then dried under a nitrogen stream. After this pre-cleaning, the bare gold surface of the chip was obtained by immersing the chip for 5 min in freshly prepared piranha solution [H_2O_2:H_2SO_4 1:5] pre-cooled to room temperature for 15 min under a magnetic-induction stirrer. Immediately after, the chip was immersed in water to remove residual piranha solution, and rinsed again with water (150 mL), followed by 96% ethanol (50 mL), then dried under a nitrogen stream. After that, the chip was placed horizontally under the biohazard safety VBH sterile hood and exposed to the germicidal UV light of the hood for 1 h.

The cleaned chip was then either used immediately for in-situ surface coating or used ex-situ for thiol-mediated immobilization of the SH-glyco-derivatives. For this, inside the sterile hood the chip was again rinsed with water (150 mL) and 96% ethanol (50 mL) and placed in a homemade sealed parafilm box.The dried surface of the chip was covered with freshly prepared SH-glyco-derivative solution (800 μg/mL) diluted in 50% ethanol, and left for 24 h on a circular shaker in the dark. Then the surface was gently rinsed with water (50 mL) and 96% ethanol (5 mL), dried under a nitrogen stream, and re-inserted into the chip housing. All the above steps (chip cleaning and ligand immobilization) were carried out in succession.

Table 1
Characterization by DLS of citrate and glycol-capped GNPs.

Gold Nanoparticles	Hydrodynamic diameter (nm)	Polydispersity index	ζ-Potential (mV)
Citrate-GNPs	33 ± 9	0.201± 0.03	-26± 5
Man-GNPs	28 ± 7	0.173 ± 0.03	-19±2
Glc-GNPs	29± 7	0.177 ± 0.01	-9± 2

2.6. SPR binding assays

All the SPR analyses were done with the Proteon XPR36 SPR. The running and dilution buffer was TBST with Ca^{2+} 10 mM Tris buffer [pH 7.4], with 150 mM NaCl, 0.005% Tween-20 and 1.2 mM $CaCl_2$.

For initial binding studies different concentrations of rhMBL (0.125–20 nM) were injected for 300 s at a rate of 30 μL/min, over chips coated directly with different SH-glyco-derivatives, as described above. Representative sensorgrams (i.e., the time course of the SPR signal in resonance units (RU)) were obtained from parallel spots of the SPR chip surfaces (Fig. S6).

For inhibition studies, 1 μg/mL (5 nM) rhMBL was pre-incubated with monovalent mannose (10 mM and 30 mM) or M9 glycan (100–200 μM) for 1 h, as indicated, at 25 °C on an orbital shaker, and the solutions were then injected over the chip, for 150–300 s at 30 μL/min.

In another set of experiments, 1 μg/mL rhMBL was preincubated with or without Man-$EG_6C_{11}S$-functionalized GNPs (25, 12.5, 6.25 μg/mL) or Glc-$EG_6C_{11}S$-functionalized GNPs (25 μg/mL) for 1 h at 25 °C on an orbital shaker. The solutions were injected over the chip surface for 5 min at 30 μL/min or centrifuged at 13000 rpm (16.1 rcf) for 25 min at 4 °C to precipitate the NPs, and the supernatants were injected as above.

To evaluate the binding of native MBL, 50-fold-diluted human serum was preincubated with or without of Man-$EG_6C_{11}S$- or Glc-$EG_6C_{11}S$-functionalized GNPs (25 μg/mL) for 1 h at 25 °C on an orbital shaker. Then the solutions were centrifuged at 13000 rpm (16.1 rcf) for 25 min at 4 °C, to precipitate the NPs, and the supernatants were injected over the chip surface, for 800 s at 30 μL/min. In parallel we used MBL-depleted human serum with or without the addition of rhMBL.

The injection of diluted sera was immediately followed by injection of anti-hMBL 3E7 antibody (10 μg/mL at a rate of 30 μL/min for to specifically recognize the MBL captured by the immobilized sugars.

3. Results

3.1. In-situ functionalization of the SPR chip is not efficient

First, we attempted to immobilize the SH-glyco-derivatives directly in the SPR instrument, i.e. flowing the SH-molecules over the bare gold surface. This would allow different SH-molecules to be immobilized in parallel lanes of the same sensor chip (Fig. S6) and would give more control of the level of immobilization.

Fig. S7A shows the sensorgrams obtained when flowing Man-$EG_6C_{11}S$ (800 μg/mL) or mercaptoethanol 1 M (used as a control SH-molecule) on the bare gold surface for 980 s, indicating that both of them could be immobilized at high levels. The highest signal of Man-$EG_6C_{11}S$ was lower than with mercaptoethanol, despite the higher MW, indicating that the number of immobilized Man-$EG_6C_{11}S$ molecules is about 15 times lower than the number of immobilized mercaptoethanol molecules.

Fig. S7B shows the binding signals of rhMBL on the prepared surfaces. The response was good on the Man-$EG_6C_{11}S$-immobilized surface but not on the mercaptoethanol-immobilized surface; however, rhMBL binding was even greater on the unfunctionalized bare gold, probably due to the cysteine groups of the protein. We hypothesized that mercaptoethanol efficiently coated the whole surface, while the immobilization of Man-$EG_6C_{11}S$ was not so efficient, leaving some unfunctionalized gold-surface to which rhMBL can bind.

To confirm this, the Man-$EG_6C_{11}S$-immobilized surface was subjected to an intermediate flow of mercaptoethanol for 980 s, followed by rhMBL injection. In this condition, the binding of rhMBL was substantially lower (green), supporting the notion that in-instrument immobilization of Man-$EG_6C_{11}S$ is not sufficient to saturate the whole surface.

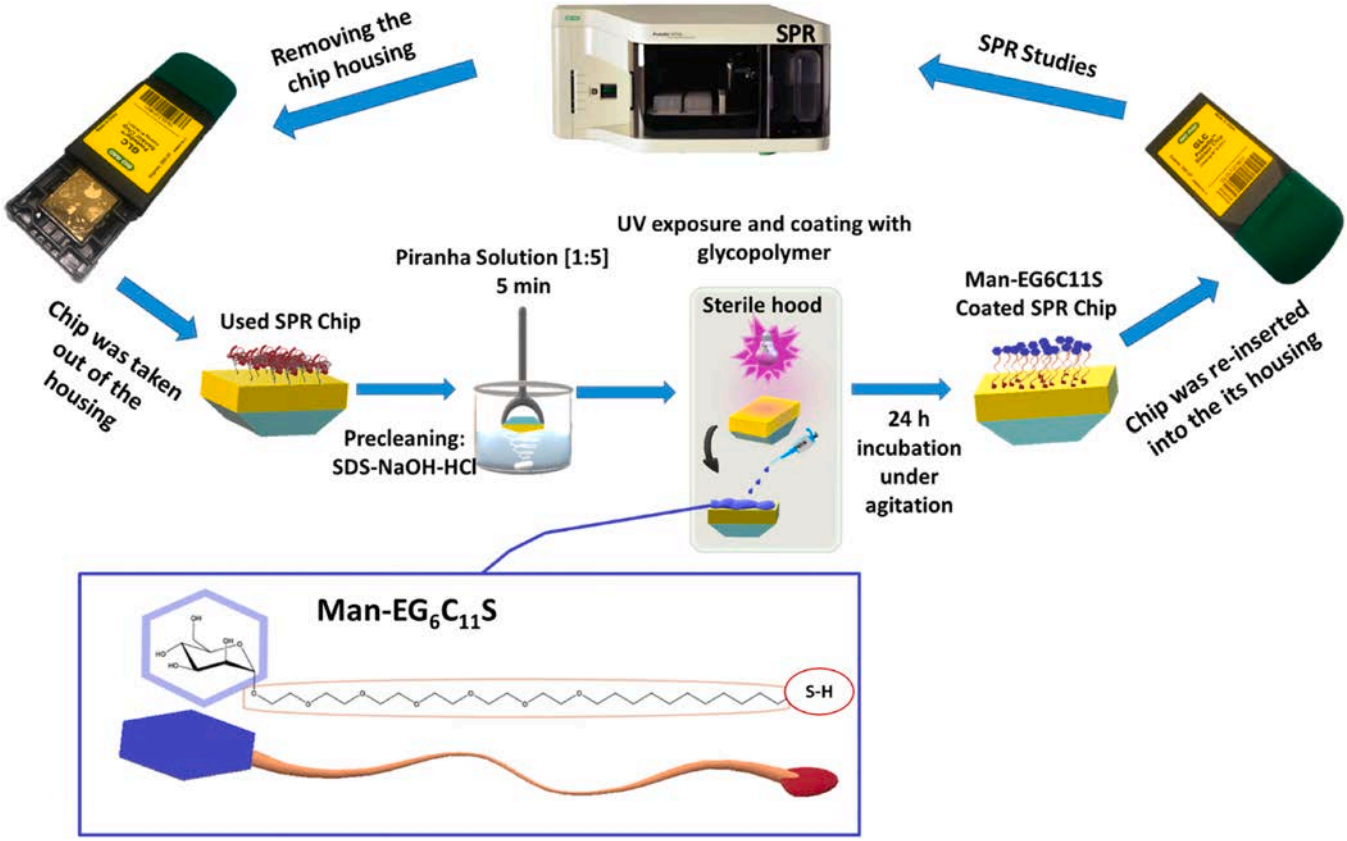

Fig. 1. Diagramatic scheme of piranha/UV cleaning and the chip surface coating cycle.

3.2. Ex-situ functionalization of the SPR chip is efficient and reproducible

To overcome the low functionalization efficiency, we immobilized the SH-glyco-derivatives on the bare gold surface outside the SPR instrument. This meant the incubation time could be extended to 24 h, with the aim of allowing a complete functionalization. After this incubation, the chip is inserted into the SPR instrument (Fig. 1) to evaluate the MBL-binding to the functionalized surfaces.

To be feasible, this approach needed a suitable method for chip regeneration. We therefore tested different cleaning strategies to remove the immobilized ligands, e.g. dextran matrices or SH-glyco-derivatives, and identified the combination of immersion in piranha solution followed by exposure to UV as the best (Fig. 2A).

Fig. 2 B shows the binding of flowing rhMBL (10 nM) over a cleaned surface functionalized with Man-$EG_6C_{11}S$. This binding is highly reproducible in six parallel spots of the same chip (see the dots in Fig. S6), indicating homogeneous functionalization. However, to exclude that this rhMBL binding also involves binding to the gold surface, we prepared a new chip functionalized with Glc-$EG_6C_{11}S$, as a negative control. In this condition, there was not any binding of flowing rhMBL (Fig. 2C), confirming that after functionalization with these glyco-derivatives no residual bare gold surface is available for rhMBL and the binding shown in Fig. 2B is specific for mannose moieties.

Further studies were carried out to evaluate the performances of the same chip after sequential regenerations. Fig. 2D shows that this enabled us to completely remove the immobilized Man-$EG_6C_{11}S$ (compare panels D and E), while maintaining the surface properties for subsequent functionalizations (compare panels E and F, in which rhMBL binding is reinstated after regeneration and functionalization with Man-$EG_6C_{11}S$).

3.3. Characterization of the binding properties of Man-$EG_6C_{11}S$-coated surface in buffer and serum

Using the conditions for surface cleaning and functionalization described above, we characterized the binding properties of the Man-$EG_6C_{11}S$-coated surface.

Fig. 3 A shows the concentration-dependent binding of rhMBL to Man-$EG_6C_{11}S$ previously immobilized on a cleaned GLC chip. The K_D was 0.46 ± 0.03 μg/mL, calculated by a fitting of all the sensorgrams in Fig. 3A with the Langmuir equation. Assuming a MW of rhMBL of 230 kDa (i.e. trimers of structural monomers, each made up of three identical 25.5 kDa polypeptide chains [29]), the estimated K_D is 2.3 ± 0.13 nM (mean±SD of six different detection spots) as in the literature [30]. Results were very similar on a pre-cleaned GLM chip (1.6 ± 0.4 nM) (Fig. S8). The mean K_D from twelve injections of different concentrations of rhMBL over eight piranha/UV cleaned chips (up to four times) functionalized with Man- $EG_6C_{11}S$ is 2.3 ± 0.33 nM (association rate constant k_{on} 7.4 ± 0.7×10^5 $M^{-1}s^{-1}$; dissociation rate constant k_{off} 1.3 ± 0.2×10^{-3} s^{-1}).

The Man-$EG_6C_{11}S$-coated surface did not bind Soybean-agglutinin and rh-Ficolin1 (Fig. 3B), in agreement with literature data showing no binding of these lectins to mannose [31,32].

We then investigated whether the Man-$EG_6C_{11}S$-coated surface also binds native MBL. We injected human serum, diluted 50 times to reduce non-specific binding due to other serum proteins. Diluted MBL-depleted serum was tested in parallel to estimate this non-specific binding. Fig. 4A shows the clear MBL-dependent binding, although there was also significant MBL-independent binding. To specifically visualize the MBL-dependent binding, we added a second injection with an anti-MBL antibody, immediately after the serum. The antibody injection specifically detected the MBL-dependent binding, since the signal was negligible for MBL-depleted serum (Fig. 4B).

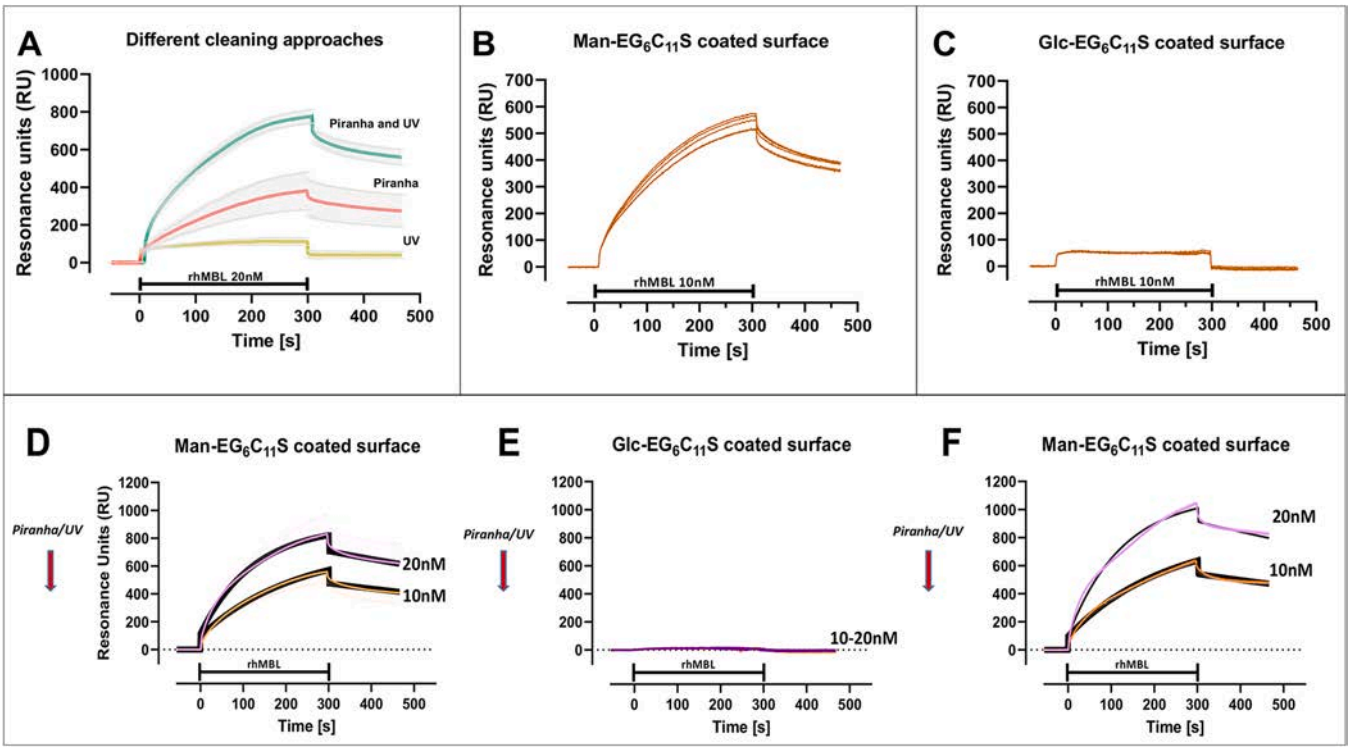

Fig. 2. The cleaning method and its reproducibility. (A) Comparison of different cleaning approaches to reclaim the used SPR chip. Chips were cleaned as indicated, and functionalized with Man-$EG_6C_{11}S$ outside of the SPR instrument. rhMBL (20 nM) was flowed for 300 s as indicated. The data show the sensorgrams (i.e., time course of SPR signal in RU) expressed as mean±SD of five detection spots of the same chip. (B-C) SPR signals obtained flowing rhMBL (10 nM) over a surface coated with Man-$EG_6C_{11}S$ (B) or Glc-$EG_6C_{11}S$. The data show the sensorgrams obtained in the five different detection spots. (D-E-F) Sensorgrams obtained on the same chip after sequential cleaning with piranha/UV, surface coating outside the SPR instrument as indicated, and injection of rhMBL. The data show the sensorgrams expressed as mean±SD of six detection spots of the same chip (for clarity only one side of SD is shown). Black lines show the fitting of the sensorgrams in panel D and F, with a common estimated KD of 2.3 nM (the small difference in the absolute RU values was accounted for small difference in the estimated Rmax, left free in the fitting, as expected for different immobilizations).

To check for quenching of the MBL detection due to the matrix, we added rhMBL to MBL-depleted serum and compared the binding signal with those in buffer. Diluted serum had only a slight (13%) quenching effect (Fig. 4C,D).

3.4. Recognizing MBL inhibitors in buffer

Preincubation of rhMBL for 1 h in buffer with 10 or 30 mM mannose (1.8 and 5.4 mg/mL) resulted in concentration-dependent inhibition of rhMBL binding to Man-$EG_6C_{11}S$-coated surface, with IC50 5.1 mM (95% CI 5.45 ± 2.35 mM) (~ 1 mg/mL) (Fig. 5A).

We then tested a glycan carrying nine mannose residues (M9), screened after 1 h preincubation of rhMBL in buffer (Fig. 5B). M9 was tested at 100 and 200 μM, corresponding to 0.18 and 0.36 mg/mL. The glycan inhibited rhMBL binding to the Man-$EG_6C_{11}S$-coated surface with an estimated IC50 of 175 μM (0.33 mg/mL). These data indicate that this oligo-mannose glycan increases the affinity of MBL by about 30 times, presumably due to the multivalency effect.

We also investigated the inhibitory effect of Man- or Glc-coated NPs. These NPs were synthesized starting from citrate-capped GNPs with a core diameter of 14.1 ± 2.1 nm (Fig. S3). The citrate-GNPs and glyco-GNPs were fully characterized by TEM and UV-Vis (Figs. S3–4) and by DLS in order to determine their hydrodynamic diameter and check their colloidal stability by measuring their ζ-potentials (see Table 1).

For evaluation of the inhibitory effect of Man- or Glc-coated GNPs, we preincubated rhMBL in TBST/Ca^{2+} buffer for 1 h with different concentrations of GNPs. In initial experiments we injected the mixture, including GNPs, over the functionalized sensor surface. These data indicated a relevant binding of GNPs themselves on the surface (Fig. S9A), which made it necessary to perform a second injection with anti-MBL antibody (Fig. S9B). Although suggesting an inhibitory effect of GNPs (Fig. S9) the possibility that MBL bound to the GNPs might still be recognized by the antibody would make the interpretation of the results difficult. Since our aim here was to see whether GNPs actually bind MBL, we centrifuged the solution in order to pellet GNPs with bound MBL, injecting the supernatants (containing unbound rhMBL) over Man-EG6C11S-coated surfaces. Fig. 5C shows that Man-coated NPs reduced the rhMBL-dependent binding signal in a concentration-dependent manner, with an extrapolated IC50 of 1.1 μg /mL (95% CI 0.2–3.3 μg /mL) whereas Glc-coated NPs had a much smaller inhibitory effect, with IC50 > 25 μg /mL. The very small amount of NPs with an inhibitory effect (1.1 μg /mL) indicates that the avidity effect markedly raises the affinity of these multivalent mannose-based ligands of MBL by 2–3 orders of magnitude.

3.5. Recognizing MBL inhibitors in serum

Studies were carried out to see whether the GNP also inhibits MBL binding in serum, i.e. to assess whether the protein corona possibly formed on NPs in serum affects their ability to bind MBL. We pre-incubated Man- or Glc-coated GNPs (6.25 μg/mL) in 50-fold diluted human serum for 1 h. The solutions were then centrifuged to pellet NPs, and the supernatants (containing unbound MBL) injected over the Man-$EG_6C_{11}S$-coated surface (Fig. 6A). To clearly dissect the MBL-dependent binding, we added a second injection with an anti-MBL antibody, after the one with serum. Fig. 6B shows that Man-coated NPs completely inhibited the binding of native MBL (blue), while Glc-coated NPs had negligible inhibitory effect (Fig. 6B, green).

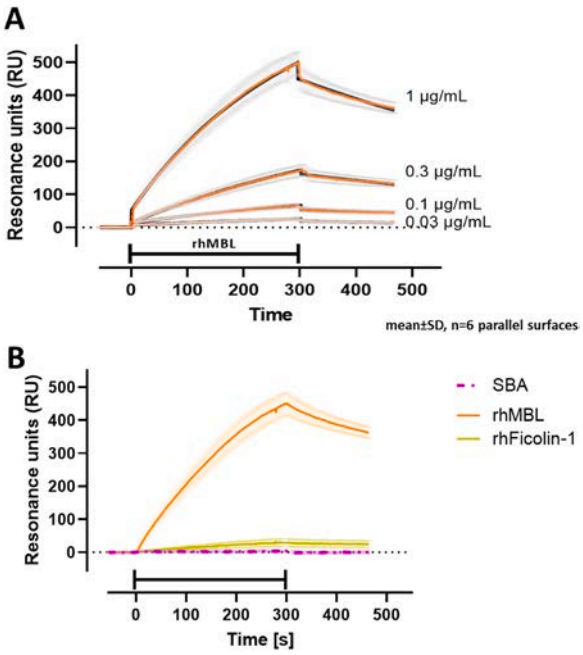

Fig. 3. Binding properties of the Man-$EG_6C_{11}S$-coated SPR chip surface. (A) Concentration-dependent binding of rhMBL obtained by simultaneous injections of four dilutions of rhMBL (0.03–1 µg/mL). Panel A shows the variability of the sensorgrams obtained in six detection spots (SD shown as shaded area) with the fitting (black lines) obtained using the Langmuir equation results in a KD of 0.46 µg/mL. (B) Binding specificity was evaluated by injecting a fixed concentration (1 µg/mL) of different lectins: rhMBL (orange), rhFicolin-1 (green), Soybean Agglutinin (SBA) (pink) over Man-$EG_6C_{11}S$-coated SPR chip surface.

4. Discussion

We developed and characterized a new SPR assay for in vitro screening of compounds inhibiting MBL binding to carbohydrate patterns. The putative inhibitor is preincubated with MBL and these solutions are flowed over a sensor chip exposing a suitable carbohydrate pattern. With this experimental design we aim to identify compounds to inhibit the binding of blood MBL to the sugar moieties exposed on cell membranes (see in graphic abstract). This method has been successfully applied to two novel materials, a glycan carrying nine mannose residues and a mannose-coated nanoparticle. These multivalent mannosylated constructs were produced to interfere with the multivalent interactions underlying MBL binding to carbohydrate patterns [30,33], and behaved as potent MBL inhibitors.

For the development and characterization of the method, we considered different critical issues such as the need for chip functionalization capable of specific and sensitive recognition of MBL (both recombinant and native in biological matrices) and the need for a robust and convenient screening assay.

For the functionalization of the chip surface, we directly coupled thiol-glyco-derivatives on the chip gold surface, in order to prepare a self-assembled monolayer (SAM) in only one step. We employed (-$EG_6C_{11}SH$) as previously investigated by their SAM formation [27,34] with two different end-sugar groups, mannose for its affinity to MBL and glucose as a negative control for the assay.

At first, we tried to functionalize the chip surface inside the SPR instrument by flowing the SH-molecules over a bare gold surface. This protocol would have had important advantages: to control the amount of immobilized molecule by measuring the SPR signal in real time and to immobilize different SH-molecules in each parallel strip of the same sensor chip. Unfortunately, this approach was not successful, probably because the exposure of the bare gold to the flowing Man-$EG_6C_{11}SH$ was too short to saturate the whole surface, and gave rise to significant non-

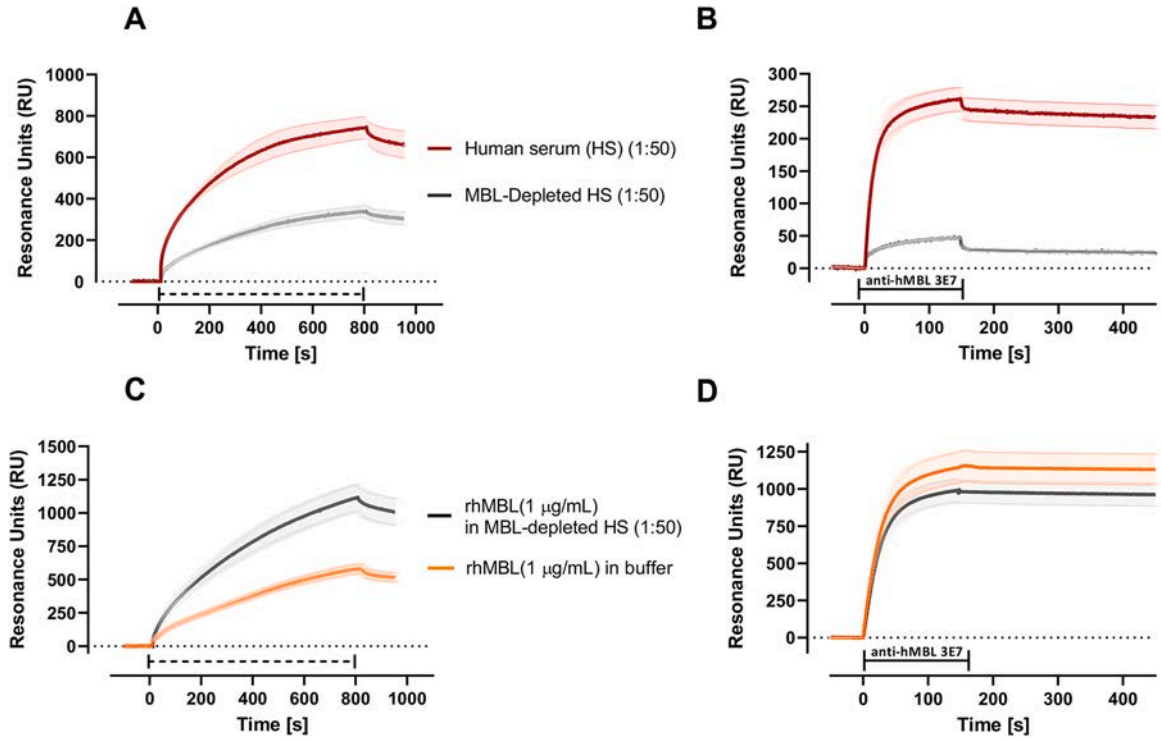

Fig. 4. Capture of native or recombinant hMBL by Man-$EG_6C_{11}S$-coated chip surface. The graphs show representative sensorgrams, i.e., the time course of the surface plasmon resonance signal in resonance units (RU). (A) Human serum (HS) or MBL-depleted HS was injected for 800 s at the rate of 30 µg/mL over chip surfaces coated with Man-$EG_6C_{11}S$. (B) MBL-dependent binding was then determined by sequential injections of anti-hMBL 3E7 antibody (10 µg/mL) shortly after the sera. (C) Injection of rhMBL (1 µg/mL) in TBST/ Ca^{2+} buffer or in MBL-depleted HS over Man-$EG_6C_{11}S$. (D) MBL-dependent binding determined by sequential injections of 3E7 antibody (10 µg/mL) shortly after rhMBL. All sera were diluted 1:50 in TBST/ Ca^{2+}. Data show the mean±SD of the sensorgrams obtaind in six detections spots.

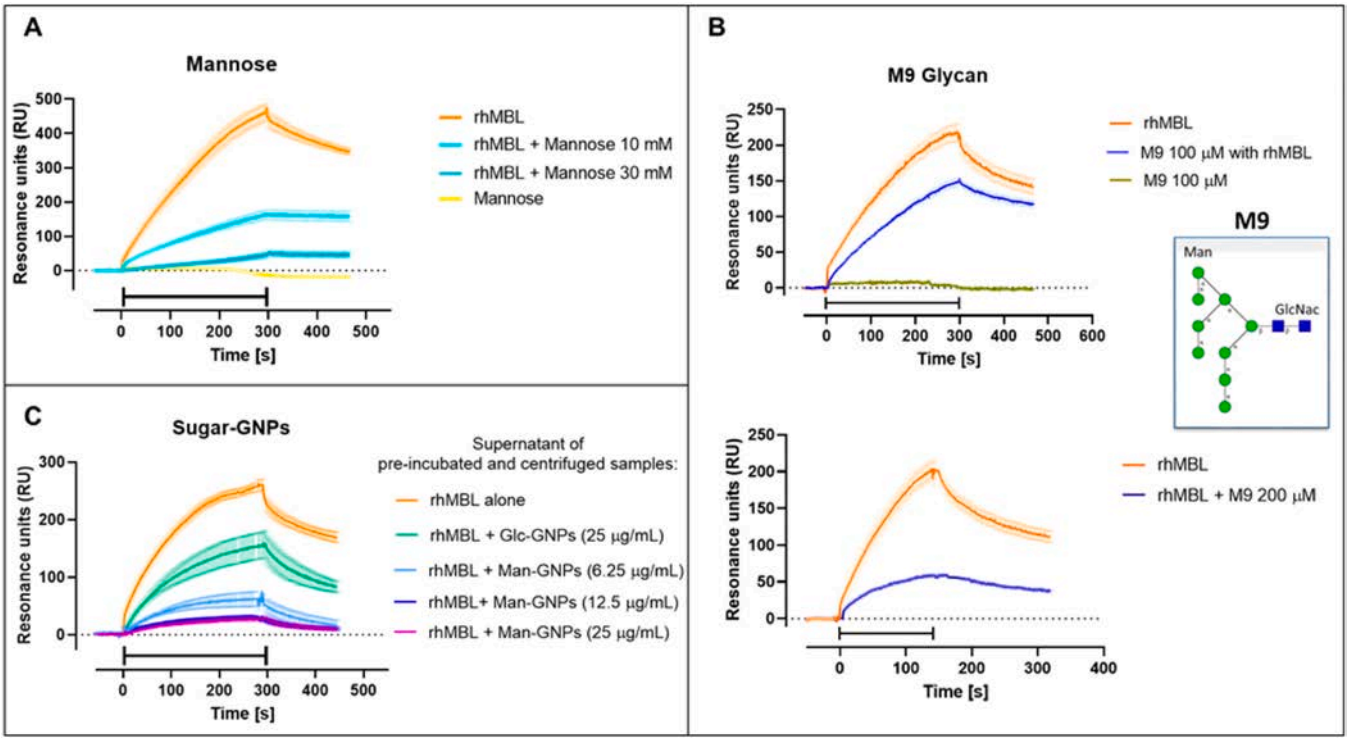

Fig. 5. Proof of principle for screening different inhibitors of MBL binding to a Man-$EG_6C_{11}S$-coated SPR chip surface. rhMBL binding after preincubation of (A) monovalent mannose (10 and 30 mM) (blue) B) M9 Glycan (100–200 µM) (blue), or rhMBL alone (orange). (C) Mannose-functionalized GNPs (6.5–25 µg/mL) (blue), or glucose-functionalized GNPs (25 µg/mL) (green). Data show the mean±SD of the sensorgrams obtaind in 5–6 detections spots.

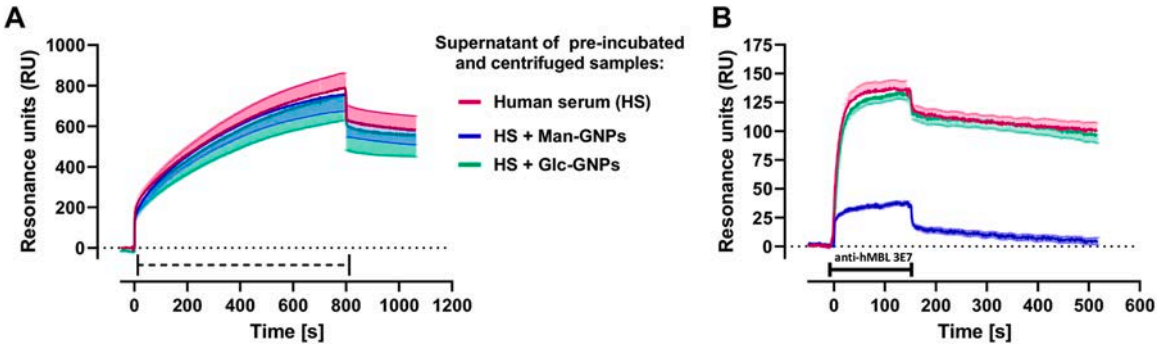

Fig. 6. Inhibition of MBL binding by glyco-capped GNPs in human serum. HS (1:50) was preincubated with and without Man-$EG_6C_{11}S$ (blue) and Glc-$EG_6C_{11}S$ (green) coated GNPs (6.25 µg/mL) for 1 h, and precipitated by centrifugation (25 min). Only the supernatants were injected simultaneously for 800 s over parallel channels of the Man-$EG_6C_{11}S$ coated SPR chip. (A) Specific MBL binding determined by sequential injections of anti-hMBL 3E7 antibody (10 µg/mL) shortly after the injection of sera. (B) Each sensorgram shows the mean of six parallel sensor spots; SD is indicated as shaded area (one side only for clarity).

specific binding of MBL to bare gold. Backfilling the surface with an excess of mercaptoethanol – a smaller thiolated molecule – considerably reduced the non-specific binding but also failed to produce an MBL-specific signal, suggesting that the immobilization of Man-$EG_6C_{11}SH$ was insufficent. This is consistent with literature data [35–37] indicating that the formation of well-organized and complete SAM requires exposure of the chip to the solution for hours. Unfortunately, hours-long flow of the ligands within the instrument was not feasible, since the flowing solution could not be recycled and therefore an excessive amount of material would have been required. We therefore carried out the surface functionalization outside the SPR instrument.

Besides the preparation of SAMs by gold-thiol interaction, we also developed a method for efficient and complete cleaning/regeneration of a previously used chip, allowing multiple uses. This was accomplished by sequential cleaning with piranha solution followed by UV exposure [38]. While several studies [35,39,40] have used piranha solution for chip cleaning, to our knowledge there are no data on combining this process with UV exposure. We found that binding of rhMBL to a Man--$EG_6C_{11}S$-coated surface was three times higher with a chip cleaned with piranha/UV than with piranha solution only. Most probably this is due to the more efficient removal of the sulfur contamination by UV light which converts the alkylthiolates to water-soluble alkylsulfonates, that can be removed from the surface by thorough washing [38]. We also demonstrated that this cleaning/regeneration method achieves complete removal of the immobilized SH-glycopolymer, while maintaining the surface properties for subsequent functionalization, hence very good reproducibility after different regeneration/functionalization steps (e.g. Fig. 2D-F). This protocol can be applied to different SH-ligands and therefore it might be useful in different research areas.

We found Man-$EG_6C_{11}S$ was the best MBL-capturing molecule. As expected [15], there was no binding with Glc-$EG_6C_{11}S$, immobilized in the same manner, indicating that the whole surface is covered by the

glycopolymer. Other, different sugars can be added to the -$EG_6C_{11}S$ moiety in order to have ligands specific for the different lectins, making this a highly flexible tool.

We also confirmed the specificity of the Man-dependent MBL binding, since no binding to Man-$EG_6C_{11}S$ was observed with other lectins, with different sugar selectivity [15]. This is a further proof that the chip surface was sufficiently coated with Man-$EG_6C_{11}S$ to prevent non-specific adsorption of proteins. Furthermore, the binding of MBL to immobilized Man-$EG_6C_{11}S$ was concentration-dependent and the sensorgram analysis indicated a K_D of 2.3 nM. This high-affinity binding suggests a multivalent interaction, i.e. each MBL molecule binds – through its different CRD domains – to different mannose residues on the chip [41].

This novel method also proved able to measure native MBL in human serum, which is a very important feature not accomplished with our previous approach [24]. Since human serum gives quite a high non-specific signal, a second injection with an anti-MBL antibody was required to specifically recognize the serum MBL captured during the first injection.

The most important application of this new SPR assay is the possibility of screening MBL inhibitors with an experimental design resembling the in vivo condition. In fact, the putative ligands are incubated with MBL in solution (mimicking what occurs in blood, since MBL is a circulating protein), to look for their effect in preventing MBL binding to chip-exposed sugars (mimicking the carbohydrate patterns exposed on endothelial cells). Inhibitor screening can be carried out with rhMBL in buffer or with human serum (i.e. native hMBL). It is important here to highlight an important advantage of SPR even other assays (e.g. mannan immunoassay) [15] carried out at equilibrium. In fact, the long incubation of MBL-containing solution in sugar-coated microtiter wells may reduce the binding between the inhibitor and MBL, due to the equilibrium shift induced by the high-affinity binding of free MBL to immobilized sugars. This potential artifact, leading to underestimation of the compound's inhibitory effect, is minimized during the very short flow of plasma over the mannose-coated SPR surface. Another worthwhile advantage of the SPR assay is that it does not need any labeled reagent and uses less antibody than for microtiter wells.

We applied this approach to monomeric mannose, which inhibited MBL binding with an IC50 in the mM range, as expected [42,43]. A new oligo-mannose glycan was also purified and tested which had three times higher inhibitory potency than monomeric mannose, presumably because of the multivalency effect.

Finally, we developed, characterized and tested new polymannosylated NPs, i.e. Man-$EG_6C_{11}S$-coated NPs, which proved to be extremely potent as hMBL inhibitors, both in buffer (rhMBL) and serum (native hMBL), with a potency at least 2–3 orders of magnitude higher than monomeric mannose, presumably a result of the multivalence effect provided by the coated NPs [44,45]. As expected, Glc-$EG_6C_{11}S$--coated NPs had much less potency (> 25-fold).

The SPR-based screening assay described here suggests that novel polymannosylated glycan and Man-$EG_6C_{11}S$-coated NPs are promising MBL inhibitors. These in vitro results offer a basis for testing the protective properties of these molecules/NPs in the more expensive and time-consuming studies in cells and animal models of MBL-mediated injuries.

Funding

This project has received funding from the European Union's Horizon 2020 research and innovation programme under the Marie Skłodowska-Curie grant agreement No 814236.

CRediT authorship contribution statement

Gizem Erol: Conceptualization, Methodology, Formal analysis, Investigation, Visualization, Writing – original draft, Writing – review & editing. **Patricia Perez Schmidt:** Resources, Investigation, Writing – review & editing. **Alessia Pancaro:** Resources, Investigation, Writing – review & editing. **Javier M. Melo Diaz:** Resources, Investigation, Writing – review & editing. **Africa G. Barrientos:** Resources, Writing – review & editing. **John Porter:** Resources, Writing – review & editing. **Laura Polito:** Resources, Investigation, Writing – review & editing. **Michal Szymonik:** Resources, Investigation, Writing – review & editing. **Inge Nelissen:** Resources, Writing – review & editing. **Daniel I. R. Spencer:** Resources, Writing – review & editing. **Arianna Piotti:** Methodology, Writing – review & editing. **Marten Beeg:** Methodology, Writing – review & editing. **Maria-Grazia De Simoni:** Conceptualization, Writing – review & editing, Funding acquisition. **Stefano Fumagalli:** Conceptualization, Writing – review & editing, Funding acquisition. **Marco Gobbi:** Conceptualization, Methodology, Formal analysis,Writing – original draft, Writing – review & editing, Supervision, Funding acquisition.

Declaration of Competing Interest

The authors declare the following financial interests/personal relationships which may be considered as potential competing interests, Daniel I. R. Spencer reports a relationship with Ludger Ltd that includes: employment. The authors based at Ludger Ltd work in commercializing analytical assays for use in the field of glycomics and the analysis of biopharmaceuticals.

Acknowledgement

The authors wish to thank Mrs. Judith Baggott for English stylistic editing.

Appendix A. Supporting information

Supplementary data associated with this article can be found in the online version at doi:10.1016/j.snb.2022.131661.

References

[1] E. Duverger, Carbohydrate-lectin interactions assessed by surface plasmon resonance, Biochimie 85 (2003) 167–179, https://doi.org/10.1016/S0300-9084(03)00060-9.
[2] W. Vornholt, M. Hartmann, M. Keusgen, SPR studies of carbohydrate–lectin interactions as useful tool for screening on lectin sources, Biosens. Bioelectron. 22 (2007) 2983–2988, https://doi.org/10.1016/j.bios.2006.12.021.
[3] W. Wang, B. Soriano, Q. Chen, Glycan profiling of proteins using lectin binding by surface plasmon resonance, Anal. Biochem. 538 (2017) 53–63, https://doi.org/10.1016/j.ab.2017.09.014.
[4] A. Varki, Biological roles of glycans, Glycobiology 27 (2017) 3–49, https://doi.org/10.1093/glycob/cww086.
[5] D. Ricklin, G. Hajishengallis, K. Yang, J.D. Lambris, Complement - a key system for immune surveillance and homeostasis, Nat. Immunol. 11 (2010) 785–797, https://doi.org/10.1038/ni.1923.
[6] D. Ricklin, E.S. Reis, J.D. Lambris, Complement in disease: a defence system turning offensive, Nat. Rev. Nephrol. 12 (2016) 383–401, https://doi.org/10.1038/nrneph.2016.70.
[7] M.N. Busche, V. Pavlov, K. Takahashi, G.L. Stahl, Myocardial ischemia and reperfusion injury is dependent on both IgM and mannose-binding lectin, Am. J. Physiol. Heart Circ. Physiol. 297 (2009) H1853–H1859, https://doi.org/10.1152/ajpheart.00049.2009.
[8] M.C. Walsh, T. Bourcier, K. Takahashi, L. Shi, M.N. Busche, R.P. Rother, S. D. Solomon, R.A.B. Ezekowitz, G.L. Stahl, Mannose-binding lectin is a regulator of inflammation that accompanies myocardial ischemia and reperfusion injury, J. Immunol. 175 (2005) 541–546, https://doi.org/10.4049/jimmunol.175.1.541.
[9] B. de Vries, S.J. Walter, C.J. Peutz-Kootstra, T.G.A.M. Wolfs, L.W.E. van Heurn, W. A. Buurman, The mannose-binding lectin-pathway is involved in complement activation in the course of renal ischemia-reperfusion injury, Am. J. Pathol. 165 (2004) 1677–1688, https://doi.org/10.1016/S0002-9440(10)63424-4.
[10] M.L. Hart, K.A. Ceonzo, L.A. Shaffer, K. Takahashi, R.P. Rother, W.R. Reenstra, J. A. Buras, G.L. Stahl, Gastrointestinal ischemia-reperfusion injury is lectin complement pathway dependent without involving C1q, J. Immunol. 174 (2005) 6373–6380, https://doi.org/10.4049/jimmunol.174.10.6373.
[11] L. Neglia, S. Fumagalli, F. Orsini, A. Zanetti, C. Perego, M.-G.De Simoni, Mannose-binding lectin has a direct deleterious effect on ischemic brain microvascular

endothelial cells, J. Cereb. Blood Flow. Metab. 40 (2020) 1608–1620, https://doi.org/10.1177/0271678×19874509.
[12] F. Orsini, P. Villa, S. Parrella, R. Zangari, E.R. Zanier, R. Gesuete, M. Stravalaci, S. Fumagalli, R. Ottria, J.J. Reina, A. Paladini, E. Micotti, R. Ribeiro-Viana, J. Rojo, V.I. Pavlov, G.L. Stahl, A. Bernardi, M. Gobbi, M.-G.De Simoni, Targeting mannose-binding lectin confers long-lasting protection with a surprisingly wide therapeutic window in cerebral ischemia, Circulation 126 (2012) 1484–1494, https://doi.org/10.1161/CIRCULATIONAHA.112.103051.
[13] D. De Blasio, S. Fumagalli, L. Longhi, F. Orsini, A. Palmioli, M. Stravalaci, G. Vegliante, E.R. Zanier, A. Bernardi, M. Gobbi, M.-G.De Simoni, Pharmacological inhibition of mannose-binding lectin ameliorates neurobehavioral dysfunction following experimental traumatic brain injury, J. Cereb. Blood Flow. Metab. 37 (2017) 938–950, https://doi.org/10.1177/0271678×16647397.
[14] L. Longhi, F. Orsini, D. De Blasio, S. Fumagalli, F. Ortolano, M. Locatelli, N. Stocchetti, M.-G. De Simoni, Mannose-binding lectin is expressed after clinical and experimental traumatic brain injury and its deletion is protective, Crit. Care Med. 42 (2014) 1910–1918, https://doi.org/10.1097/CCM.0000000000000399.
[15] S. Hansen, S. Thiel, A. Willis, U. Holmskov, J.C. Jensenius, Purification and characterization of two mannan-binding lectins from mouse serum, J. Immunol. 164 (2000) 2610–2618, https://doi.org/10.4049/jimmunol.164.5.2610.
[16] V.I. Pavlov, Y.S. Tan, E.E. McClure, L.R. La Bonte, C. Zou, W.B. Gorsuch, G.L. Stahl, Human mannose-binding lectin inhibitor prevents myocardial injury and arterial thrombogenesis in a novel animal model, Am. J. Pathol. 185 (2015) 347–355, https://doi.org/10.1016/j.ajpath.2014.10.015.
[17] P.J. Sandoval, J. Santiago, In vitro analytical approaches to study plant ligand-receptor interactions1 [OPEN], Plant Physiol. 182 (2020) 1697–1712, https://doi.org/10.1104/pp.19.01396.
[18] A. Saftics, S. Kurunczi, B. Peter, I. Szekacs, J.J. Ramsden, R. Horvath, Data evaluation for surface-sensitive label-free methods to obtain real-time kinetic and structural information of thin films: a practical review with related software packages, Adv. Colloid Interface Sci. 294 (2021), 102431, https://doi.org/10.1016/j.cis.2021.102431.
[19] R.L. Rich, D.G. Myszka, Higher-throughput, label-free, real-time molecular interaction analysis, Anal. Biochem. 361 (2007) 1–6, https://doi.org/10.1016/j.ab.2006.10.040.
[20] M. Canovi, J. Lucchetti, M. Stravalaci, F. Re, D. Moscatelli, P. Bigini, M. Salmona, M. Gobbi, Applications of surface plasmon resonance (SPR) for the characterization of nanoparticles developed for biomedical purposes, Sensors 12 (2012) 16420–16432, https://doi.org/10.3390/s121216420.
[21] M. Beeg, L. Diomede, M. Stravalaci, M. Salmona, M. Gobbi, Novel approaches for studying amyloidogenic peptides/proteins, Curr. Opin. Pharmacol. 13 (2013) 797–801, https://doi.org/10.1016/j.coph.2013.05.010.
[22] H. Šípová, J. Homola, Surface plasmon resonance sensing of nucleic acids: a review, Anal. Chim. Acta 773 (2013) 9–23, https://doi.org/10.1016/j.aca.2012.12.040.
[23] M. Beeg, A. Nobili, B. Orsini, F. Rogai, D. Gilardi, G. Fiorino, S. Danese, M. Salmona, S. Garattini, M. Gobbi, A surface plasmon resonance-based assay to measure serum concentrations of therapeutic antibodies and anti-drug antibodies, Sci. Rep. 9 (2019), https://doi.org/10.1038/s41598-018-37950-4.
[24] M. Stravalaci, D. De Blasio, F. Orsini, C. Perego, A. Palmioli, G. Goti, A. Bernardi, M.-G. De Simoni, M. Gobbi, A new surface plasmon resonance assay for in vitro screening of mannose-binding lectin inhibitors, J. Biomol. Screen. 21 (2016) 749–757, https://doi.org/10.1177/1087057116637563.
[25] R. Rajagopalan, V.P. Salvi, J. Chr, Jensenius, N. Rawal, New insights on the structural/functional properties of recombinant human mannan-binding lectin and its variants, Immunol. Lett. 123 (2009) 114–124, https://doi.org/10.1016/j.imlet.2009.02.013.
[26] Á.G. Barrientos, J.M. de la Fuente, T.C. Rojas, A. Fernández, S. Penadés, Gold Glyconanoparticles: synthetic polyvalent ligands mimicking glycocalyx-like surfaces as tools for glycobiological studies, Chem. Eur. J. 9 (2003) 1909–1921, https://doi.org/10.1002/chem.200204544.
[27] O. Martínez-Ávila, K. Hijazi, M. Marradi, C. Clavel, C. Campion, C. Kelly, S. Penadés, Gold *Manno* -Glyconanoparticles: multivalent systems to block HIV-1 gp120 binding to the lectin DC-SIGN, Chem. Eur. J. 15 (2009) 9874–9888, https://doi.org/10.1002/chem.200900923.
[28] A. Silvestri, V. Zambelli, A.M. Ferretti, D. Salerno, G. Bellani, L. Polito, Design of functionalized gold nanoparticle probes for computed tomography imaging: design of tailored engineered AuNPs as CT contrast agents, Contrast Media Mol. Imaging 11 (2016) 405–414, https://doi.org/10.1002/cmmi.1704.
[29] P. Garred, F. Larsen, J. Seyfarth, R. Fujita, H.O. Madsen, Mannose-binding lectin and its genetic variants, Genes Immun. 7 (2006) 85–94, https://doi.org/10.1038/sj.gene.6364283.
[30] L.C. Gjelstrup, J.D. Kaspersen, M.A. Behrens, J.S. Pedersen, S. Thiel, P. Kingshott, C.L.P. Oliveira, N.M. Thielens, T. Vorup-Jensen, The role of nanometer-scaled ligand patterns in polyvalent binding by large mannan-binding lectin oligomers, J. Immunol. 188 (2012) 1292–1306, https://doi.org/10.4049/jimmunol.1103012.
[31] L. Guo, S. Chao, P. Huang, X. Lv, Q. Song, C. Wu, Y. Pei, Z. Pei, A universal photochemical method to prepare carbohydrate sensors based on perfluorophenylazide modified polydopamine for study of carbohydrate-lectin interactions by QCM Biosensor, Polymers 11 (2019) 1023, https://doi.org/10.3390/polym11061023.
[32] C. Honoré, S. Rørvig, T. Hummelshøj, M.-O. Skjoedt, N. Borregaard, P. Garred, Tethering of Ficolin-1 to cell surfaces through recognition of sialic acid by the fibrinogen-like domain, J. Leukoc. Biol. 88 (2010) 145–158, https://doi.org/10.1189/jlb.1209802.
[33] C. Müller, G. Despras, T.K. Lindhorst, Organizing multivalency in carbohydrate recognition, Chem. Soc. Rev. 45 (2016) 3275–3302, https://doi.org/10.1039/C6CS00165C.
[34] H. Guesmi, N.B. Luque, E. Santos, F. Tielens, Does the S−H bond always break after adsorption of an alkylthiol on Au(111)? Chem. Eur. J. 23 (2017) 1402–1408, https://doi.org/10.1002/chem.201604574.
[35] Z. Altintas, Surface plasmon resonance based sensor for the detection of glycopeptide antibiotics in milk using rationally designed nanoMIPs, Sci. Rep. 8 (2018), https://doi.org/10.1038/s41598-018-29585-2.
[36] V. Spampinato, M.A. Parracino, R. La Spina, F. Rossi, G. Ceccone, Surface analysis of gold nanoparticles functionalized with thiol-modified glucose SAMs for biosensor applications, Front. Chem. 4 (2016), https://doi.org/10.3389/fchem.2016.00008.
[37] G.M. Whitesides, J.K. Kriebel, J.C. Love, Molecular engineering of surfaces using self-assembled monolayers, Sci. Prog. 88 (2005) 17–48, https://doi.org/10.3184/003685005783238462.
[38] C.G. Worley, R.W. Linton, Removing sulfur from gold using ultraviolet/ozone cleaning, J. Vac. Sci. Technol. A 13 (1995) 2281–2284, https://doi.org/10.1116/1.579510.
[39] J.M. Lee, H.K. Park, Y. Jung, J.K. Kim, S.O. Jung, B.H. Chung, Direct immobilization of protein G variants with various numbers of cysteine residues on a gold surface, Anal. Chem. 79 (2007) 2680–2687, https://doi.org/10.1021/ac0619231.
[40] K. Park, J.M. Lee, Y. Jung, T. Habtemariam, A.W. Salah, C.D. Fermin, M. Kim, Combination of cysteine- and oligomerization domain-mediated protein immobilization on a surface plasmon resonance (SPR) gold chip surface, Analyst 136 (2011) 2506, https://doi.org/10.1039/c0an00966k.
[41] W.K. Eddie Ip, K. Takahashi, R. Alan Ezekowitz, L.M. Stuart, Mannose-binding lectin and innate immunity, Immunol. Rev. 230 (2009) 9–21, https://doi.org/10.1111/j.1600-065X.2009.00789.x.
[42] H. Jensenius, D.C.G. Klein, M. van Hecke, T.H. Oosterkamp, T. Schmidt, J. C. Jensenius, Mannan-binding lectin: structure, oligomerization, and flexibility studied by atomic force microscopy, J. Mol. Biol. 391 (2009) 246–259, https://doi.org/10.1016/j.jmb.2009.05.083.
[43] A. Miller, A. Phillips, J. Gor, R. Wallis, S.J. Perkins, Near-planar solution structures of mannose-binding lectin oligomers provide insight on activation of lectin pathway of complement, J. Biol. Chem. 287 (2012) 3930–3945, https://doi.org/10.1074/jbc.M111.320341.
[44] C.R. Becer, The glycopolymer code: synthesis of glycopolymers and multivalent carbohydrate–lectin interactions, Macromol. Rapid Commun. 33 (2012) 742–752, https://doi.org/10.1002/marc.201200055.
[45] G. Yilmaz, C.Remzi Becer, Glyconanoparticles and their interactions with lectins, Polym. Chem. 6 (2015) 5503–5514, https://doi.org/10.1039/C5PY00089K.

Gizem Erol is a titled pharmacist from Ege University, Turkey and currently a Ph.D. candidate in the NanoCarb project under Marie Sklodowska-Curie Actions- Innovative Training networks. She is carrying out her Ph.D. research at Mario Negri Institute for Pharmacological Research and enrolled in the Experimental Neuroscience Ph.D. Program of the University of Milano-Bicocca, Italy. Her research focuses on identification of glyco-coated nanoparticles as inhibitors for specific lectins to develop novel therapeutic strategies for ischemic injuries.

Patricia Perez Schmidt is a Ph.D. degree candidate at University of the Basque Country and University of Milano-Bicocca. She is research fellow at Istituto di Scienze e Tecnologie Chimiche "Giulio Natta" (SCITEC) of the National Research Council - CNR of Italy. Her researches focus on the synthesis and characterization of glyco-nanopartiles.

Alessia Pancaro is a Marie Curie Ph.D. fellow working at VITO (Belgium) on the development of gold nanorods conjugated with synthetic glycopolymers as a diagnostic biosensing platform for the detection of lectin biomarkers of stroke patients. She obtained a M.Sc in Molecular and Industrial biotechnology at the Università degli Studi di Napoli Federico II.

Javier M. Melo Diaz is an ESR under the Nanocarb consortium, working at Ludger Ltd on production of glycan standards.

Africa G. Barrientos was MidaCore Tecnology Platform Lead and Head of Laboratory of Tech Transfer and R&D in Midatech Pharma. Her main research has been focused on gold glyconanoparticles, from the basic research and applications to the translation to the industrial pharmaceutical processes. Currently, she is R&D Project Manager and Senior Researcher in i + Med, a company specialized in the development of nanohydrogels, controlled release systems and medical devices.

Dr John Porter was Chemistry Group Leader at Midatech Pharma plc. He is a medicinal chemist by training and has research interests in the inhibition of protein-protein interactions and the conformational effects of small molecules binding to proteins as well as the synthesis and use of nanoparticles.

Laura Polito received her Ph.D. degree from University of Milan (Italy). She is currently research scientist at the Istituto di Scienze e Tecnologie Chimiche "Giulio Natta" (SCITEC) of the National Research Council - CNR of Italy. Her researches focus on the synthesis and functionalization of nanomaterials for bioapplications.

Michal Szymonik is a researcher at the Flemish Institute for Technological Research (VITO). His main research interest is the development of point-of-care biosensor technologies for medical diagnostics, incorporating various sensing modalities and biorecognition elements.

Dr. Inge Nelissen is team leader at the Health department of VITO nv. Her research and development interests are in assays and nano-enabled technologies for health diagnostics.

Daniel I. R. Spencer obtained his doctorate in the study of mucin-type O-glycosylation involvement in epithelial cancers. He is head of a research and development team at Ludger Ltd. which specializes in analytical assays for studying both patient cohorts and also glycoprotein biopharmaceuticals. His team also advances the production of glycan and glycopeptide standards for use in both research and quality assurance.

Arianna Piotti is research fellow in the laboratory of "Pharmacodynamics and Pharmacokinetics" (PD-PK lab) of the Mario Negri Institute for Pharmacological Research (IRCCS), Italy. Her research interests includes the development and validation of binding and analytical assays on SPR and HPLC/MS-MS, recently applied for example to the analysis of biomarkers of sepsis.

Marten Beeg received his Ph.D. in pharmacology from the Open University in 2010 and is currently a senior scientist at the Mario Negri Institute for Pharmacological Research. His research interests include biomolecular reactions and interaction responsible for protein aggregation and the use of analytical assays based on label free techniques to study biomolecular therapeutics.

Maria-Grazia De Simoni is the Head of Inflammation and Nervous System Diseases Laboratory at Mario Negri Insitute, Milan. Her main scientific interests include the study the pathogenesis of acute brain injury. She contributed to clarify the role of the complement system in brain injury, to identify MBL as a novel therapeutical target and to develop selective inhibitory strategies.

Stefano Fumagalli, Ph.D., is the head of the Unit of Pathophysiology of Cerebrovascular Functions at the Istituto di Ricerche Farmacologiche Mario Negri IRCCS, Milan, Italy. His research focuses on complement system-mediated vascular alterations following stroke.

Marco Gobbi earned a Master degree in Pharmacy at the University of Milan in 1989. From 2010 he is the the head of the laboratory of "Pharmacodynamics and Pharmacokinetics" (PD-PK lab) in the Department of Biochemistry and Molecular Pharmacology at the Mario Negri Institute for Pharmacological Research. Among the main activities of the lab (https://www.marionegri.it/laboratories/laboratory-of-pharmacodynamics-and-pharmacokinetics) are the development and application of new analytical assays to measure drugs, proteins, therapeutic antibodies and endogenous biomarkers.